Volume 2 | Number 42 | 14 November 2014 | Pages 17693–18150

Journal of Materials Chemistry A

Materials for energy and sustainability

www.rsc.org/MaterialsA

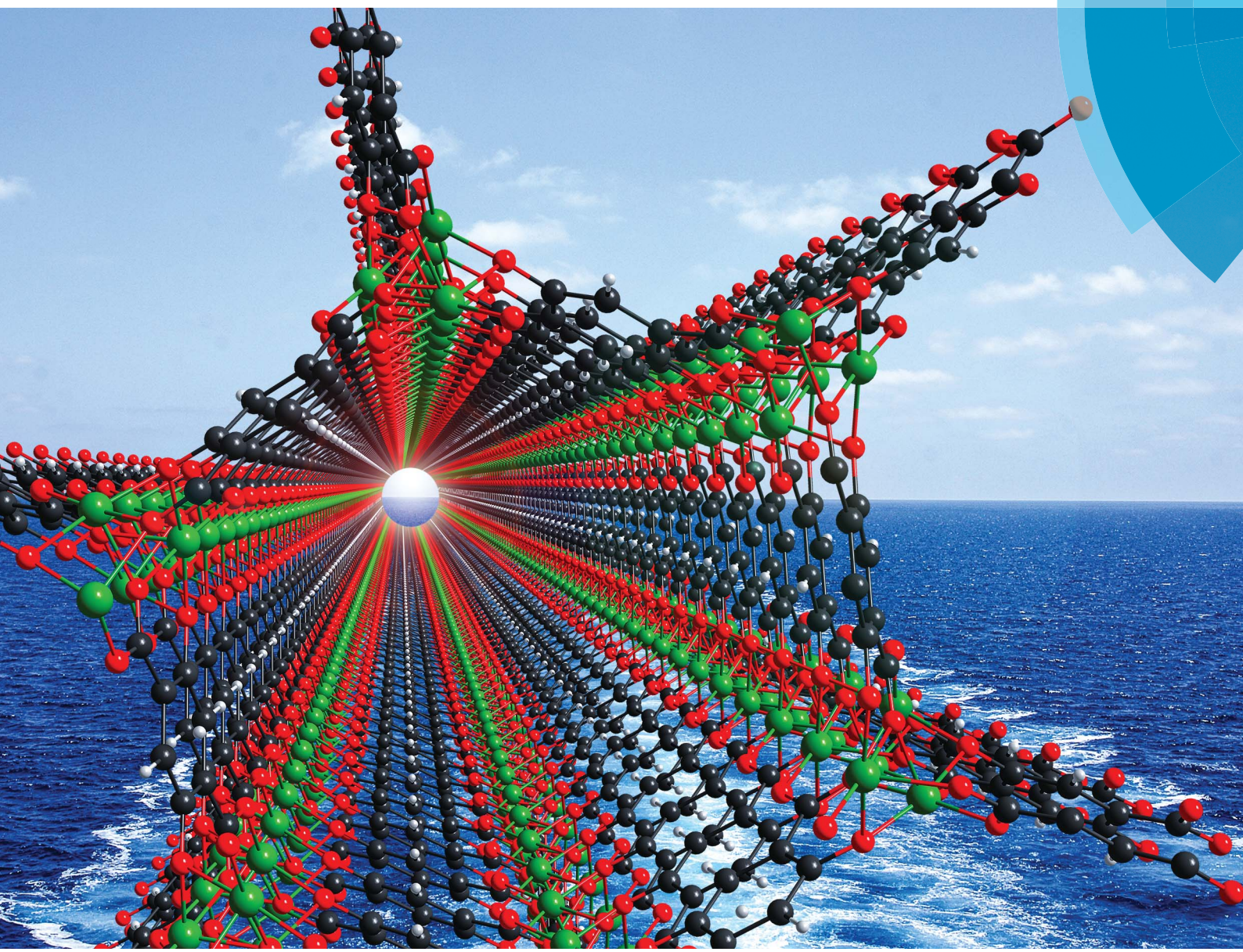

ISSN 2050-7488

ROYAL SOCIETY OF CHEMISTRY

PAPER

Elsje Alessandra Quadrelli *et al.*

A water-based and high space-time yield synthetic route to MOF Ni_2(dhtp) and its linker 2,5-dihydroxyterephthalic acid

Journal of Materials Chemistry A

PAPER

View Article Online
View Journal | View Issue

Cite this: J. Mater. Chem. A, 2014, 2, 17757

A water-based and high space-time yield synthetic route to MOF Ni_2(dhtp) and its linker 2,5-dihydroxyterephthalic acid†

Stéphane Cadot,[ab] Laurent Veyre,[a] Dominique Luneau,[c] David Farrusseng[d] and Elsje Alessandra Quadrelli*[a]

Received 17th June 2014
Accepted 24th July 2014

DOI: 10.1039/c4ta03066d

www.rsc.org/MaterialsA

2,5-Dihydroxyterephthalic acid (H_4dhtp) was synthesized on an 18 g scale by carboxylation of hydroquinone in molten potassium formate. The hydrated form of the Ni_2(dhtp) MOF (also known as CPO-27-Ni and MOF-74(Ni)) was obtained in 92% yield by refluxing for 1 h a water suspension of the H_4dhtp linker with an aqueous solution of nickel acetate. The ensuing characterization of the material (XRD, HRTEM, TGA, N_2 adsorption at 77 K – S_{BET} = 1233 m^2 g^{-1}) confirmed the formation of a metal–organic framework of at least equal quality to the ones obtained from the previously reported routes (CPO-27-Ni and MOF-74(Ni)), with a different morphology (namely, well-separated 1 μm platelets for the herein reported water-based route). The temperature dependence of the magnetic susceptibility was measured and satisfactorily simulated assuming a Heisenberg ($H = -2J\Sigma S_i S_{i+1}$) ferromagnetic intrachain interaction (J = +8.1 cm^{-1}) and an antiferromagnetic interchain interaction (J' = −1.15 cm^{-1}). Overall, the reaction in water appears to follow easily distinguishable steps, the first being the deprotonation of H_4dhtp by an acetate counterion, leading to a soluble nickel adduct of the linker, *en route* to the MOF self-assembly.

Introduction

Metal–Organic Frameworks (MOFs) have received considerable attention over the past decade, especially in the field of gas purification and storage as well as catalysis and drug delivery.[1] The growing interest in these materials has recently led to the first industrial production of MOFs with the ton-scale synthesis of aluminum fumarate (Basolite A520®) at BASF facilities[2] which is a promising candidate for methane storage and delivery. This transfer to industrial production has been achieved, *inter alia*, through the development of a water-based route, reducing both production costs and environmental impact while increasing the production rates. Unfortunately, entirely water-based MOF syntheses are still very limited.[2–6]

Among the wide diversity of MOFs, the M_2(dhtp) series (dhtp = dobdc = 2,5-dioxido-1,4-benzenedicarboxylate [O_2C–$C_6H_2O_2$–CO_2]$^{4-}$; M = Mg, Mn, Fe, Co, Ni or Zn),[7] called CPO-27-M (CPO = Coordination Polymer of Oslo) or MOF-74(M), has been extensively studied because of its 1D microporous hexagonal channel structure with calibrated pores at 12 Å which allow an optimal interaction between the walls of the solid and guest molecules. In fact, M_2(dhtp) offers a permanent porosity upon solvent removal, displaying strong adsorption centers at the penta-coordinated open metal sites (see Scheme 1 for M = Ni) which allow the selective adsorption/desorption of a wide diversity of molecules without loss of porosity.[8–10] In particular the nickel member of the M_2(dhtp) series, which is highly tolerant towards moisture[11] and oxygen,[12] is able to reversibly adsorb sulfur-containing molecules like H_2S[13] or thiophene,[14] and selectively adsorb CO and CO_2 over CH_4 and H_2[9,10] and CO_2 over N_2 even under 3% relative humidity[15] while the efficiency of this separation using Mg_2(dhtp) or zeolites is much more affected by only a trace amount of water.[16,17] Most strikingly, the methane storage capacity of Ni_2(dhtp) is among the highest reported for MOFs (214 cm^3 (STP) cm^{-3} at 25 °C, 35 bars),[18] which makes it a very promising candidate for adsorption and/or separation applications. Ni_2(dhtp) is also active as a Lewis-type catalyst[19] and its application for delivering an anticancer drug[20] as well as its use in antimicrobial NO-delivering patches[21] has been reported.

Overall, MOF syntheses, there included Ni_2(dhtp) synthetic routes reported so far[12,22,23] (see the Results section below for

[a]Equipe Chimie Organométallique de Surface, C2P2 – UMR 5265 (CNRS – Université Lyon 1 – CPE Lyon), CPE Lyon, 43 Boulevard du 11 Novembre 1918, 69616 Villeurbanne Cedex, France. E-mail: quadrelli@cpe.fr

[b]CEA, LETI, MINATEC Campus, 17 rue des Martyrs, 38054 Grenoble Cedex 9, France

[c]Laboratoire des Multimatériaux et Interfaces – UMR 5615 (Université Claude Bernard Lyon 1), Campus de La Doua, 69622 Villeurbanne Cedex, France

[d]Institut de Recherche sur la Catalyse et l'Environnement de Lyon (IRCELYON), 2 Av. Albert Einstein, 69626 Villeurbanne cedex, France

† Electronic supplementary information (ESI) available: Experimental and simulated nitrogen adsorption and desorption isotherms at 77 K and thermogravimetric analysis (TGA) under N_2 and O_2 of Ni_2(dhtp) as well as the XRD diffraction pattern of the intermediate isolated along the synthesis described in the main text. See DOI: 10.1039/c4ta03066d

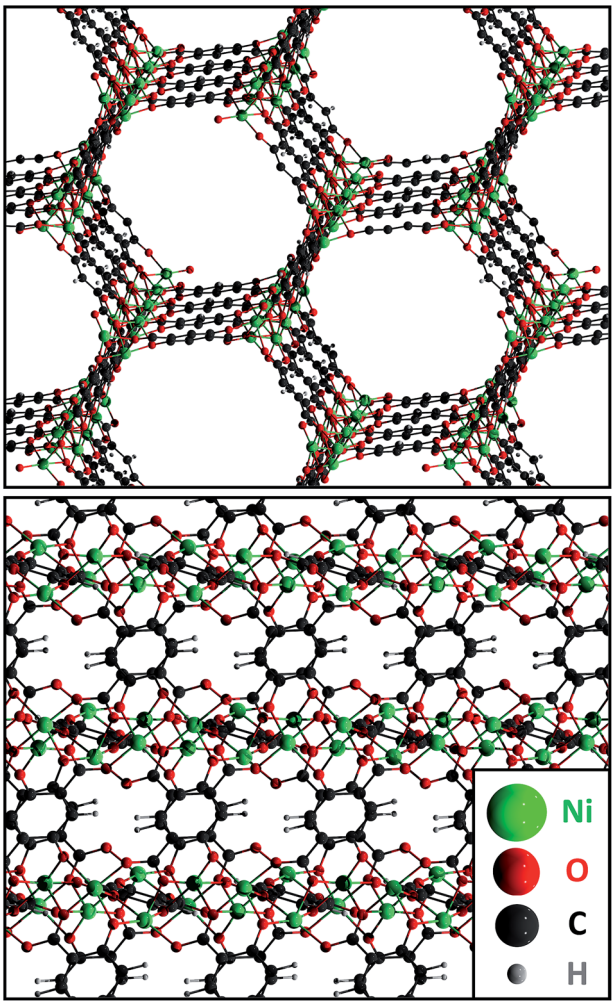

Scheme 1 Representation of the fully desolvated Ni_2(dhtp) structure[22] showing the hexagonal 1D channels (upper picture: view towards the (113) plane, lower picture: view towards the (−120) plane).

details), require high dilution factors which imply large amounts of organic solvents, low production rates and strong environmental impact. This is mainly ascribed to the difficulty in finding a good solvent for both the metal salt and the organic linker. Therefore, non-optimized small-scale lab syntheses as described in the literature have usually space-time yields (STY) between 0.1 and 1 kg per m^3 per day or even lower.[10] While the reaction time has been reduced by one order of magnitude using ultrasound or microwave heating,[24] the minimization of solvent usage is still a goal to attain with a STY larger than 500 kg per m^3 per day. Beyond this, the development of water-based routes for MOF synthesis would strongly facilitate their industrialization. Indeed, organic solvents are more difficult to use at industrial levels because they shall be handled in specific non-flammable areas, while water is a cheap, safe and more easily post-treatable solvent.

Here we report for the first time the synthesis of Ni_2(dhtp) in water with high space-time yield. We carefully demonstrate the quality of the obtained Ni_2(dhtp) by a series of characterization in short and long ranges, as well as its porous structure and not yet reported magnetic properties. In addition, we describe a synthesis method for the H_4dhtp linker in a single step from hydroquinone (which is a bulk chemical) using a cheap and organic solvent-free procedure. Indeed, 2,5-dihydroxyterephthalic acid is distributed on a gram scale by different chemical suppliers at a price of about $15 per gram. Although it does not represent the price at the industrial level, it strongly limits its synthesis on a kg scale for demonstration purposes.

Results and discussion

Two different synthetic routes have been reported for the isomorphous family of M_2(dhtp), both of them requiring organic solvents: tetrahydrofuran (THF) for the CPO-27 material originated from SINTEF's work in Oslo[22] and dimethylformamide (DMF) (or DMF–water or DMF–water–ethanol mixtures) for the MOF-74[23] developed by Yaghi's group. The general procedure consists of mixing an aqueous solution of the metal salt with a solution of 2,5-dihydroxyterephthalic acid in the appropriate organic solvent inside a Teflon-lined autoclave, followed by heating at the appropriate temperature (*ca.* 100–110 °C) for 2–3 days. The use of dimethylformamide generally reduces both temperature and reaction time[25] but the resulting MOF then have to be washed several days with methanol because of the strong coordination of DMF molecules to the nickel atoms in the framework, which prevents simple removal by vacuum treatment. If the tetrahydrofuran–water mixture is used, a relatively large amount of solvent is required as well as long reaction time: in a typical procedure,[12] three days and a temperature of 110 °C were necessary to produce 6.46 g of CPO-27-Ni (4.10 g expected after complete water removal) from 100 ml of a THF/water (1 : 1) mixture.

The procedure described here for the synthesis of Ni_2(dhtp) entails only concentrated aqueous solution under atmospheric pressure, without the addition of organic co-solvent at any point of the procedure.

H_4dhtp synthesis

2,5-Dihydroxyterephthalic acid has been directly synthesized in good yields from the inexpensive hydroquinone using an organic solvent-free procedure (see Scheme 2), derived from a patented process[26] and adapted for the laboratory-scale experiment by replacing pressurized CO_2 with an atmospheric-pressure CO_2 stream. Preformed potassium formate has also been replaced by its *in situ* generation from K_2CO_3 and HCOOH to yield the molten salt reaction medium. The yellow crystalline 2,5-dihydroxyterephthalic acid can be conveniently recovered by

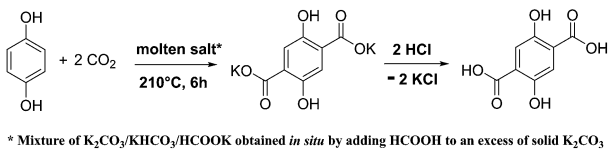

Scheme 2 Reaction scheme for the synthesis of 2,5-dihydroxyterephthalic acid by dicarboxylation of hydroquinone.

filtration after acidification of the reaction crude and washing with water, and used directly for the MOF synthesis.

Ni_2(dhtp) synthesis

The procedure for Ni_2(dhtp) synthesis consists of mixing an aqueous solution of nickel(II) acetate (warmed at 80 °C to allow high concentration of the metal, typically 1 M) with a suspension containing 1.02 equivalent of 2,5-dihydroxyterephthalic acid in water (*ca.* 25 g L^{-1}). Upon adding the nickel-containing solution to the linker suspension, the reaction mixture immediately turns into a clear emerald green solution. When this solution is heated at reflux temperature, a yellow solid quickly precipitates. After 1 h refluxing, washing with water and drying at 80 °C, the final product is recovered as a yellow powder with almost full conversion with respect to the nickel salt, the limiting reagent of the procedure (calculated yield: 91.6%).

X-ray diffraction

The X-ray powder diffraction (XRD) pattern of the product after full rehydration shows a highly crystalline material (see Fig. 1 for experimental and simulated diffractograms).

The highest intensity peaks of the material obtained from the aqueous procedure are found at $2\theta = 6.8°$ and 11.8° (corresponding to $d_{hkl} = 12.99$ Å and 7.48 Å). These measurements are in good agreement with the published CPO-27-Ni crystallographic data:[22] $2\theta = 6.80°$ and 11.79°, corresponding to $d_{hkl} =$ 12.99 Å and 7.50 Å, that is the (−120) and (030) planes, respectively. The X-ray powder diffraction pattern was fitted by the Le Bail full profile fitting method[27] using the FullProf[28] and Winplotr[29] software. Fig. 1 shows good agreement between the recorded powder pattern (red) and the simulated one (black). No supplementary peaks were observed in the difference curve (blue) which confirms the purity of the obtained sample.

Permanent microporosity

The reversible N_2 adsorption and desorption performed at 77 K (see Fig. 2 and S1†) lead to specific surface areas of 1233 m^2 g^{-1} (Brunauer–Emmett–Teller (BET) method) and 1355 m^2 g^{-1} (Langmuir method), in line with the highest specific surface area of 1218 m^2 g^{-1} (BET method) reported in the literature for the CPO-27-Ni material.[12] The adsorption/desorption isotherms are satisfactorily fitted with the NLDFT simulation method[30] (see Fig. S1†), which allows us to obtain a pore size distribution plot (see the inset of Fig. 2) with a mean pore diameter of 11.7 Å, in agreement with the calculated value of 11.85 Å,[12] and an estimated pore volume of 0.823 cm^3 g^{-1}.

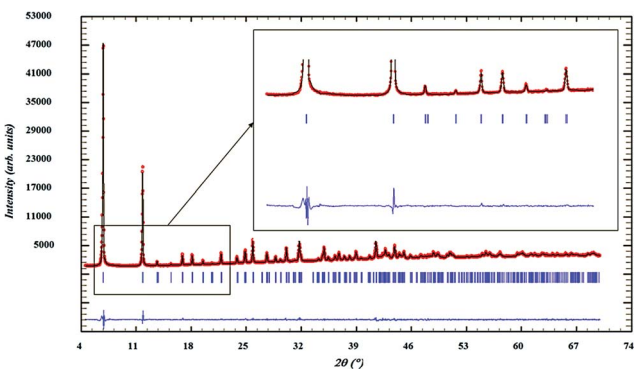

Fig. 1 View of the experimental powder XRD pattern (red dots) and the simulated one (black line) by the Le Bail method. The difference curve is shown in blue.

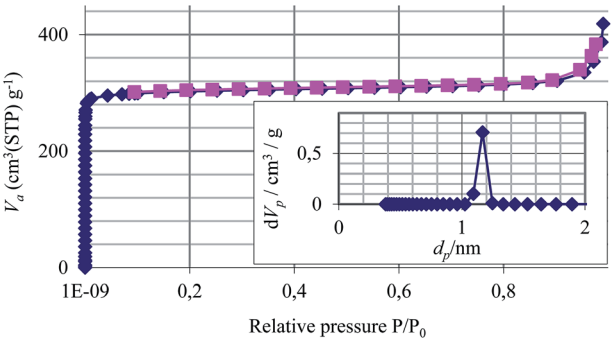

Fig. 2 Experimental N_2 adsorption (blue diamonds) and desorption (purple squares) isotherms at 77 K of Ni_2(dhtp) synthesized in aqueous solution; in the inset: calculated pore size distribution from the simulated adsorption isotherm reported in the ESI, Fig. S1.†

Magnetic susceptibility

The magnetic behavior of the Co[31] and Fe[32] members of the M_2(dhtp) isomorphous family of MOFs has already been reported, but not, to the best of our knowledge that of Ni_2(dhtp), for which only a theoretical investigation is available.[33] At room temperature, the product of the magnetic susceptibility and the temperature (χT), of a fully rehydrated Ni_2(dhtp) obtained from the water based route, is 2.67 cm^3 K mol^{-1}. Upon cooling, χT increases and reaches the maximum value of 3.57 cm^3 K mol^{-1} at 20 K and then drops abruptly below this temperature. This behavior is in agreement with the ferromagnetic coupling of nickel(II) ions ($S = 1$) along the chain running parallel to the c axis, as previously observed for Co(II) and Fe(II) analogs.[31,32] To extract the value of the magnetic interaction, the data were simulated for $[Ni_2(dhtp)(H_2O)_2]\cdot 8H_2O$ assuming Heisenberg interactions between spins ($H = -2J\Sigma S_i S_{i+1}$) using the Fisher analytical expression for the magnetic susceptibility of an infinite chain of classical spins $S = 1$ with an interchain magnetic interaction in the molecular field approximation (ZJ').[34,35] The best fit (Fig. 3A) gives a ferromagnetic intrachain interaction $J = +8.1$ cm^{-1} and an antiferromagnetic interchain interaction $J' = -1.15$ cm^{-1} with $Z = 3$ as previously suggested[32] and $g = 2.02$. A small TIP has been included (150×10^{-6} cm^{-1}). At 2 K, the magnetization *vs.* magnetic field (Fig. 3B) first increases linearly with the magnetic field. Then, around 2.8 T, a transition is observed, progressively moving towards the expected value for two nickel(II) ions ($\approx 2\ \mu_B$). This field-induced transition may be ascribed to the fact that the small antiferromagnetic interchain interactions are overtaken by the strength of the magnetic field, in line with what has already been reported for CPO-27-Co.[31]

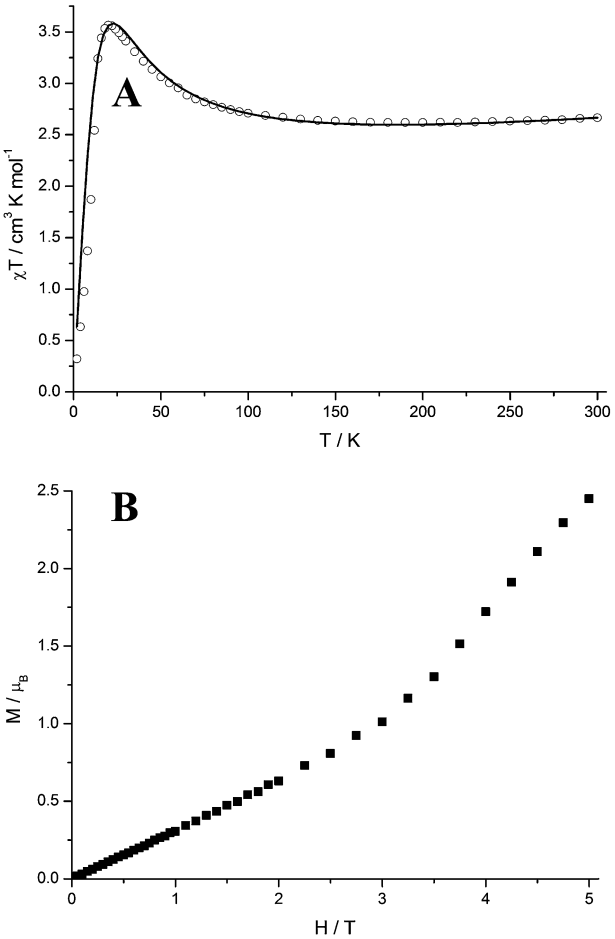

Fig. 3 (A) Temperature dependence of χT for $[Ni_2(dhtp)(H_2O)_2]\cdot 8H_2O$. The solid line is the best fit of experimental data with the parameters reported in the text; (B) magnetization curves for $[Ni_2(dhtp)(H_2O)_2]\cdot 8H_2O$.

Thermal behavior

Thermogravimetric analysis under N_2 of another aliquot of the $Ni_2(dhtp)$ material exposed to moist air at room temperature for thirty minutes displays both of the expected phenomena,[22] namely: firstly a loss of water molecules present inside the pores of the MOF or coordinated to the nickel atom, a phenomenon occurring up to 200 °C and leading to the fully dehydrated phase, $Ni_2(dhtp)$, which is stable up to 360 °C, and secondly the thermal decomposition of the MOF material (see Fig. S2A†). The water content estimated from the weight loss up to 200 °C is equivalent to about 8 molecules of water per $Ni_2(dhtp)$, suggesting an almost complete rehydration of the sample toward its fully hydrated form $[Ni_2(dhtp)(H_2O)_2]\cdot 8H_2O$ reported in the literature.[12] As already reported, the thermogram obtained under O_2 is quite similar, with decomposition occurring at lower temperature (280° *vs.* 360 °C under N_2, see Fig. S2B†).

Morphology of the $Ni_2(dhtp)$ synthesized in water

The well-formed 1D channels of the $Ni_2(dhtp)$ material obtained from the aqueous synthetic route were observed using a high-resolution transmission electron microscope (see Fig. 4A). The measured 12.5 Å distance between two contiguous lines observed in the micrograph can be explained as corresponding to the 12.99 Å spacing between two (−120) planes in the CPO-27-Ni crystallographic structure (see Fig. S3†).[22]

At lower magnification, the micrographs showed platelets of about 1 μm width (see the inset in Fig. 4A), distinctively different in morphology with respect to the crystallites obtained by us following the CPO-27-Ni procedure[12] (see Fig. 4B).

This lower symmetry morphology with the presence of agglomerates appears representative of the morphology induced by the CPO-27 route, based on the comparison with existing literature micrographs of CPO-27-Ni.[36] As recently reviewed,[37] the existence of a correlation between the composition of the solvent mixture and the crystallinity, or the shape of the resulting MOF crystals has already been established for some MOFs. The use of water as a co-solvent in such a strategy was directly addressed in a study on MIL-96(Al) shape-selected crystallite growth.[38] The solvent appears in most cases to act as a modulator of crystal nucleation processes. To the best of our knowledge, such a phenomenon had not yet been observed for a member of the $M_2(dhtp)$ family.

Mechanistic considerations

Substantial interest also lies in understanding the mechanism by which the MOF self-assembles from the metal ion and the

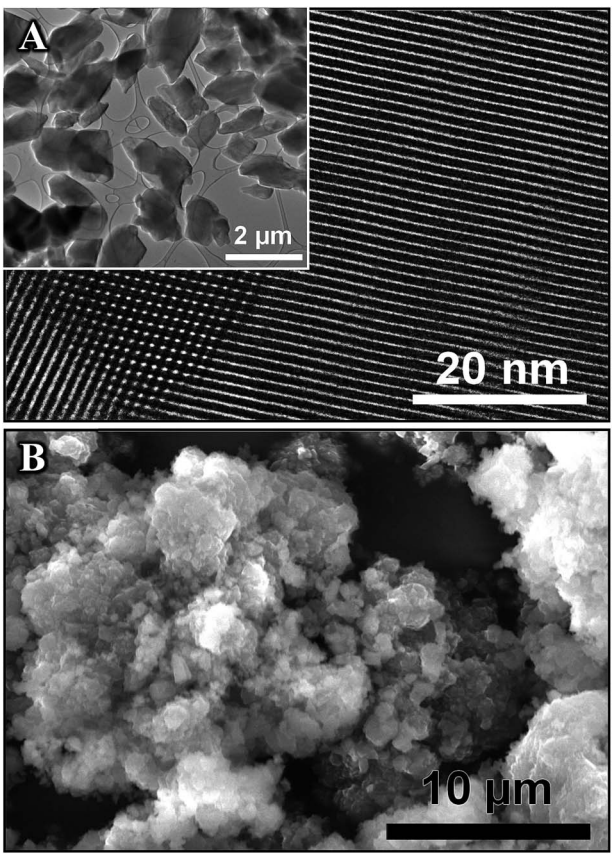

Fig. 4 A and inset) High-resolution transmission electron micrograph at different magnifications of $Ni_2(dhtp)$ obtained in water; (B) scanning electron micrograph of $Ni_2(dhtp)$ obtained in THF–water (1 : 1).[12]

linker precursor.[39] While we are unable to account for the crystallization mechanism that underpins the synthesis of Ni_2(dhtp) in water, the observation of some intermediates during the synthesis appears facilitated by the mild conditions reported here. During the synthesis, we observed the complete dissolution of the otherwise sparingly soluble acid linker at room temperature (see Fig. S4A to C†). We assign such dissolution to the deprotonation of 2,5-dihydroxyterephthalic acid (pK_a estimated at *ca.* 2.2‡) by the acetate counterion of the nickel salt present in the aqueous solution (pK_a of acetic acid = 4.76).[40] If this emerald green mother solution is stored for a few minutes at room temperature, pastel green crystals start precipitating (see Fig. S4D†) whose X-ray diffraction pattern is different from that of CPO-27-Ni (see Fig. S5†). The final MOF can be observed only when the mixture is heated above *ca.* 80 °C, and its formation is complete within 1 h if the heating is carried out at 100 °C (Fig. S4E†).

Conclusions

In conclusion, we have reported a novel synthetic route to Ni_2(dhtp): in water, under air, at atmospheric pressure, with high space-time-yield and from an affordable linker, therefore complementing this already well-remarked member of the MOF material family with an additional attractive feature. A pertinent parameter to compare the performance of the aqueous route described herein with respect to the previously reported ones in organic solvents is the space-time yield expressed in terms of isolated MOF weight/volume of solvent used/time unit.[10,41,42] While the total volume of all solvents used should be taken into consideration, the available published data allow us to calculate this value by only taking into account the volume used during the synthesis itself (and not the ones used for the washing steps). The procedure reported here yields a production rate of 28.5 g L^{-1} h^{-1}, that is a 50-fold increase with respect to the published route (0.6 g L^{-1} h^{-1} considering the weight of fully dehydrated Ni_2(dhtp)).[12] Expressed in kg per m^3 per day, the industrially pertinent unit, the space-time yield of the water-based route described here could be extrapolated to 680 kg per m^3 per day; such a figure should be considered only as a very high upper estimate, since we have tested our method only on an 18 g scale and have not included the time-intensive washing and drying steps necessary for the ton-scale batches. At the same time, such a figure bodes well for the industrial potential of this route, given the reported industrial space-time yields of 160 kg per m^3 per day for Basolite A100®, 225 kg per m^3 per day for Basolite C300® and over 300 kg per m^3 per day for Basolite M050®.[41]

Experimental section

Materials and methods

Nickel(II) acetate tetrahydrate 99%, (Sigma-Aldrich), hydroquinone (Aldrich Chemie), anhydrous K_2CO_3 (Acros), formic acid 98% (Sigma-Aldrich) and HCl 37% (VWR Chemicals) were used without further purification.

Characterization techniques

Powder X-ray diffraction data were collected from the "Centre de Diffractométrie Henri Longchambon", site CLEA, Villeurbanne, on a Bruker D8 Advance Diffractometer (Cu Kα radiation, 33 kV, 45 mA). Diffraction data were recorded in the range of 4–70° 2θ. High-resolution transmission electron micrographs were recorded at the "Centre Technologique des Microstructures", UCBL, Villeurbanne, on a Jeol 2100F transmission electron microscope. The acceleration voltage was 200 kV. Scanning electron micrographs were recorded at the "Centre Technologique des Microstructures", UCBL, Villeurbanne, on a FEI Quanta 250 FEG scanning electron microscope. Nitrogen adsorption/desorption measurements were carried out at 77 K using a BELSORB-max from BEL JAPAN system. Before N_2 adsorption, the samples were outgassed at 2.5×10^{-5} Pa; 423 K for 3 h. ^{1}H and ^{13}C liquid NMR spectra were recorded on a Bruker DSX 300 NMR spectrometer. Magnetic-susceptibility data (2–300 K) were collected with a Quantum Design MPMS SQUID magnetometer under an applied magnetic field of 0.1 T on a powdered polycrystalline sample pressed in a PTFE sample holder equipped with a piston to avoid dehydration. The magnetization isotherm was collected at 2 K between 0 and 5 T. All data were corrected with the contribution of the sample holder and diamagnetism of the sample estimated with Pascal's constants.[35] The analysis of magnetic data was carried out by simulation of χT thermal dependence including intramolecular interactions (J), intermolecular interactions (zJ') in the molecular field approximation and a temperature independent paramagnetism (TIP) according to the following expression:

$$\chi = \frac{k g_{iso}^2 F(J,T)}{12kT - 16ZJ'F(J,T)} + \mathrm{TIP}$$

where $F(J,T) = 2\dfrac{(1-u)}{(1+u)}$ and $u = \dfrac{kT}{4J} - \coth\dfrac{4J}{kT}$

Unless otherwise specified, all analyses were performed on fully rehydrated Ni_2(dhtp) samples. The rehydration procedure consisted of exposing the material (previously dried at 80 °C overnight and stored in a dry box) to water-saturated air for 24 h at room temperature.

Preparation of 2,5-dihydroxyterephthalic acid from hydroquinone

In a 500 ml 2-neck round-bottom flask equipped with a condenser, K_2CO_3 (97.7 g, 0.7 mol) was introduced. Formic acid (42.3 g, 0.9 mol) was added drop by drop under vigorous magnetic stirring, releasing a large amount of CO_2 and causing strong exothermicity. The mixture was then heated up to 210 °C, leading to a thick melt of potassium formate, bicarbonate and carbonate. The condenser was then removed and the reactor was flushed for 30 min with a continuous stream of argon. The argon line was then replaced by a 500 ml round-bottom flask filled with 300 g of dry ice. Hydroquinone (22.24 g, 0.2 mol) was added in a single portion to the melt and the condenser was

‡ Calculated using Advanced Chemistry Development (ACD/Labs) Software V11.02 (© 1994–2014 ACD/Labs).

placed back on the top of the reactor. The reaction mixture was then vigorously stirred for 6 h at 210 °C under the CO_2 stream generated by the dry ice. After 6 h, the yellow reaction mixture was dispersed in 300 ml of boiling water, leading to a suspension of white crystals in a dark-brown solution. This suspension was cooled to RT and filtered. The off-white powder obtained was finally suspended in 200 ml of water and acidified with 40 ml of HCl 37%, causing the suspension to turn canary yellow. This suspension was stirred for 1 h, filtered and washed 3 times with 50 ml portions of deionized water. The yellow product obtained was dried at 80 °C, yielding 20.8 g (105 mmol, 52.5% based on hydroquinone) of 2,5-dihydroxyterephthalic acid which was characterized by ^{1}H and ^{13}C NMR spectroscopy (see Fig. S6A and B†).

^{1}H NMR (300 MHz, DMSO-d^6) $\delta = 7.28$ ppm (2H, S); ^{13}C NMR (300 MHz, DMSO-d^6) $\delta = 170.62$; 152.26; 119.37; 117.52 ppm.

Synthesis of Ni_2(dhtp) in water

In a 500 ml round-bottom flask equipped with a condenser, a suspension of dihydroxyterephthalic acid (10.31 g, 51 mmol) in deionized water (400 ml) was heated to reflux under strong magnetic stirring (oil bath at 160 °C). In a separate flask, nickel acetate tetrahydrate (25.14 g, 100 mmol) was dissolved in deionized water (100 ml) at 80 °C. The light green nickel solution obtained was added in one portion to the boiling dihydroxyterephthalic acid suspension under continuous stirring leading almost instantaneously to a homogeneous emerald green solution. After a few minutes, a yellow precipitate started to form. The reaction mixture was further refluxed for 1 h. The final suspension was filtered and the yellow microcrystalline powder was washed three times with 100 ml portions of warm deionized water before being dried overnight at 80 °C. 17.90 g of this material were isolated and characterized by powder XRD, HRTEM and TGA. The microporosity was determined by N_2 adsorption at 77 K after activation of a 105.7 mg aliquot for 20 h at 150 °C; 5×10^{-5} mbar. The weight loss observed during this activation process was used to determine the water content in the isolated material (4.42 water molecules per Ni_2(dhtp) unit). Isolated yield: 91.6% based on 17.90 g of [Ni_2(dhtp)·4.42 H_2O].

Author contributions

The manuscript was written through contributions of all authors.

Funding sources

"Centre National de la Recherche Scientifique" (CNRS), "Ecole Supérieure de Chimie, Physique et Electronique de Lyon" (CPE Lyon) and "Université Claude Bernard Lyon 1" (UCBL) are kindly acknowledged for support.

Acknowledgements

We are grateful to Ruben Vera from the "Centre de Diffractométrie Henri Longchambon" (Université Claude Bernard Lyon 1) for XRD measurements, to Erwann Jeanneau from the "Centre de Diffractométrie Henri Longchambon" for the Le Bail refinement of the PXRD pattern, and to Ruben Checa from the "Laboratoire des Multimatériaux et Interfaces" (Université Claude Bernard Lyon 1) for magnetic susceptibility measurements.

Notes and references

1 G. Ferey, *Chem. Soc. Rev.*, 2008, **37**, 191–214.
2 M. Gaab, N. Trukhan, S. Maurer, R. Gummaraju and U. Müller, *Microporous Mesoporous Mater.*, 2012, **157**, 131–136.
3 G. Ferey, M. Latroche, C. Serre, F. Millange, T. Loiseau and A. Percheron-Guegan, *Chem. Commun.*, 2003, 2976–2977.
4 L. Bromberg, Y. Diao, H. Wu, S. A. Speakman and T. A. Hatton, *Chem. Mater.*, 2012, **24**, 1664–1675.
5 Y. Pan, Y. Liu, G. Zeng, L. Zhao and Z. Lai, *Chem. Commun.*, 2011, **47**, 2071–2073.
6 Q. Yang, S. Vaesen, F. Ragon, A. D. Wiersum, D. Wu, A. Lago, T. Devic, C. Martineau, F. Taulelle, P. L. Llewellyn, H. Jobic, C. Zhong, C. Serre, G. De Weireld and G. Maurin, *Angew. Chem., Int. Ed.*, 2013, **52**, 10316–10320.
7 S. J. Geier, J. A. Mason, E. D. Bloch, W. L. Queen, M. R. Hudson, C. M. Brown and J. R. Long, *Chem. Sci.*, 2013, **4**, 2054–2061.
8 X. Wu, Z. Bao, B. Yuan, J. Wang, Y. Sun, H. Luo and S. Deng, *Microporous Mesoporous Mater.*, 2013, **180**, 114–122.
9 E. J. García, J. P. S. Mowat, P. A. Wright, J. Pérez-Pellitero, C. Jallut and G. D. Pirngruber, *J. Phys. Chem. C*, 2012, **116**, 26636–26648.
10 G. D. Pirngruber and P. L. Llewellyn, in *Metal-Organic Frameworks – Applications from Catalysis to Gas Storage*, ed. D. Farrusseng, Wiley-VCH Verlag GmbH & Co. KGaA, 2011, pp. 99–119.
11 D. Yu, A. O. Yazaydin, J. R. Lane, P. D. C. Dietzel and R. Q. Snurr, *Chem. Sci.*, 2013, **4**, 3544–3556.
12 P. D. C. Dietzel, P. A. Georgiev, J. Eckert, R. Blom, T. Strassle and T. Unruh, *Chem. Commun.*, 2010, **46**, 4962–4964.
13 S. Chavan, F. Bonino, L. Valenzano, B. Civalleri, C. Lamberti, N. Acerbi, J. H. Cavka, M. Leistner and S. Bordiga, *J. Phys. Chem. C*, 2013, **117**, 15615–15622.
14 D. Peralta, G. Chaplais, A. Simon-Masseron, K. Barthelet and G. D. Pirngruber, *Energy Fuels*, 2012, **26**, 4953–4960.
15 J. Liu, J. Tian, P. K. Thallapally and B. P. McGrail, *J. Phys. Chem. C*, 2012, **116**, 9575–9581.
16 A. C. Kizzie, A. G. Wong-Foy and A. J. Matzger, *Langmuir*, 2011, **27**, 6368–6373.
17 J. Liu, Y. Wang, A. I. Benin, P. Jakubczak, R. R. Willis and M. D. LeVan, *Langmuir*, 2010, **26**, 14301–14307.
18 J. A. Mason, M. Veenstra and J. R. Long, *Chem. Sci.*, 2014, **5**, 32–51.
19 L. Mitchell, B. Gonzalez-Santiago, J. P. S. Mowat, M. E. Gunn, P. Williamson, N. Acerbi, M. L. Clarke and P. A. Wright, *Catal. Sci. Technol.*, 2013, **3**, 606–617.
20 S. Rojas, P. S. Wheatley, E. Quartapelle-Procopio, B. Gil, B. Marszalek, R. E. Morris and E. Barea, *CrystEngComm*, 2013, **15**, 9364–9367.

21 P. Horcajada, R. Gref, T. Baati, P. K. Allan, G. Maurin, P. Couvreur, G. Férey, R. E. Morris and C. Serre, *Chem. Rev.*, 2011, **112**, 1232–1268.
22 P. D. C. Dietzel, B. Panella, M. Hirscher, R. Blom and H. Fjellvag, *Chem. Commun.*, 2006, 959–961.
23 T. Grant Glover, G. W. Peterson, B. J. Schindler, D. Britt and O. Yaghi, *Chem. Eng. Sci.*, 2011, **66**, 163–170.
24 E. Haque and S. H. Jhung, *Chem. Eng. J.*, 2011, **173**, 866–872.
25 D. J. Tranchemontagne, J. R. Hunt and O. M. Yaghi, *Tetrahedron*, 2008, **64**, 8553–8557.
26 A. M. Reichwein and D. J. Sikkema, Akzo Nobel, N. V., 2000.
27 A. Le Bail, H. Duroy and J. L. Fourquet, *Mater. Res. Bull.*, 1988, **23**, 447–452.
28 J. Rodriguez-Carvajal, in *Collected Abstracts of Powder Diffraction Meeting*, Toulouse, France, 1990, pp. 127–128.
29 J. Rodriguez-Carvajal and T. Roisnel, *Commission on Powder Diffraction, International Union of Crystallography*, 1998, Newsletter no. 20, 35.
30 C. M. Lastoskie, *A statistical mechanics interpretation of the adsorption isotherm for the characterization of porous sorbents*, Cornell University, May 1994.
31 P. D. C. Dietzel, Y. Morita, R. Blom and H. Fjellvåg, *Angew. Chem., Int. Ed.*, 2005, **44**, 6354–6358.
32 E. D. Bloch, W. L. Queen, R. Krishna, J. M. Zadrozny, C. M. Brown and J. R. Long, *Science*, 2012, **335**, 1606–1610.
33 P. Canepa, Y. J. Chabal and T. Thonhauser, *Phys. Rev. B: Condens. Matter Mater. Phys.*, 2013, **87**, 094407.
34 M. E. Fisher, *Am. J. Phys.*, 1964, **32**, 343–346.
35 O. Kahn, *Molecular Magnetism*, Wiley-VCH, New York, NY, 1993.
36 M. Tagliabue, C. Rizzo, R. Millini, P. C. Dietzel, R. Blom and S. Zanardi, *J. Porous Mater.*, 2011, **18**, 289–296.
37 M. Sindoro, N. Yanai, A.-Y. Jee and S. Granick, *Acc. Chem. Res.*, 2013, **47**, 459–469.
38 M. Sindoro, A.-Y. Jee and S. Granick, *Chem. Commun.*, 2013, **49**, 9576–9578.
39 G. Férey, M. Haouas, T. Loiseau and F. Taulelle, *Chem. Mater.*, 2013, **26**, 299–309.
40 D. R. Lide, *CRC Handbook of Chemistry and Physics*, CRC Press, 90th edn, Boca Raton (Fla.), London, New York, 2009.
41 A. U. Czaja, N. Trukhan and U. Muller, *Chem. Soc. Rev.*, 2009, **38**, 1284–1293.
42 A. Garcia Marquez, P. Horcajada, D. Grosso, G. Ferey, C. Serre, C. Sanchez and C. Boissiere, *Chem. Commun.*, 2013, **49**, 3848–3850.